

A General Approach for All-visible-light Switching of Diarylethenes through Triplet Sensitization using Semiconducting Nanocrystals

Lili Hou (✉ lilihou@tju.edu.cn)

Tianjin University <https://orcid.org/0000-0001-9453-4924>

Wera Larsson

Chalmers University of Technology <https://orcid.org/0000-0003-1935-9884>

Stefan Hecht

DWI - Leibniz Institute for Interactive Materials <https://orcid.org/0000-0002-6124-0222>

Joakim Andreasson

Chalmers University of Technology <https://orcid.org/0000-0003-4695-7943>

Bo Albinsson

Chalmers University of Technology <https://orcid.org/0000-0002-5991-7863>

Article

Keywords:

Posted Date: December 13th, 2021

DOI: <https://doi.org/10.21203/rs.3.rs-1148200/v1>

License:  This work is licensed under a Creative Commons Attribution 4.0 International License.

[Read Full License](#)

1 **A General Approach for All-visible-light Switching of Diarylethenes through** 2 **Triplet Sensitization using Semiconducting Nanocrystals**

3 Lili Hou^{1,2,3*}, Wera Larsson¹, Stefan Hecht^{4,5}, Joakim Andréasson¹, Bo Albinsson^{1*}

4 ¹Department of Chemistry and Chemical Engineering, Chalmers University of Technology,
5 Gothenburg 412 96, Sweden.

6 ² Present Address: School of Precision Instruments and Optoelectronics Engineering, Tianjin
7 University, Tianjin 300072, China.

8 ³ Present Address: Key Laboratory of Optoelectronics Information Technology, Ministry of
9 Education, Tianjin 300072, China.

10 ⁴Department of Chemistry & IRIS Adlershof, Humboldt-Universität zu Berlin, Brook-Taylor-
11 Str. 2, 12489 Berlin, Germany.

12 ⁵DWI—Leibniz Institute for Interactive Materials & Institute of Technical and
13 Macromolecular Chemistry at RWTH Aachen University, 52074 Aachen, Germany.

14 *Corresponding author e-mails: lilihou@tju.edu.cn; balb@chalmers.se

15

16 **Abstract**

17 **Coupling semiconducting nanocrystals (NCs) with organic molecules provides an**
18 **efficient route to generate and transfer triplet excitons. These excitons can be used to**
19 **power photochemical transformations such as photoisomerization reactions using low**
20 **energy radiation. Thus, it is desirable to develop a general approach that can efficiently**
21 **be used to control photoswitches using all-visible-light aiming at future applications in**
22 **life- and material sciences. Here, we demonstrate a simple ‘cocktail’ strategy that can**
23 **achieve all-visible-light switchable diarylethenes (DAEs) through triplet energy transfer**
24 **from the hybrid of CdS NCs and phenanthrene-3-carboxylic acid, with high**
25 **photoisomerization efficiency and improved fatigue resistance. The size-tunable**
26 **excitation energies of CdS NCs make it possible to precisely match the corresponding**
27 **energy of the relevant DAE photoswitch. We demonstrate reversible all-visible-light**
28 **photoisomerization of a series of DAE derivatives both in the liquid and solid state, even**

29 **in the presence of oxygen. Our general strategy is promising for fabrication of all-visible-**
30 **light activated optoelectronic devices as well as memories, and should in principle be**
31 **adaptable to photopharmacology.**

32 **Introduction**

33 Semiconducting nanocrystals (NCs), also known as quantum dots, are quantum confined
34 inorganic crystals with high molar extinction coefficients often combined with stable and high
35 photoluminescence (PL) quantum yields¹. They have been used in a wide range of applications
36 such as light-emitting devices, bioimaging, etc²⁻⁴. The absorption and emission energies of NCs
37 critically depend on their size, which can be precisely tuned by simply varying their synthesis
38 conditions, in particular reaction temperature and time^{5,6}. Moreover, the strong spin-orbit
39 coupling of NCs mixes the singlet and triplet characters and thereby enables the harvesting of
40 triplet excitons from the NCs to surface-anchored molecules, referred to as mediators or
41 transmitters. The hybrid of NCs and appropriate mediators yields a long triplet lifetime through
42 highly efficient triplet energy transfer (TET)⁷⁻⁹. This opens up further applications of
43 NCs/molecule hybrids in high-performance light-emitting materials¹⁰ as well as solar energy
44 converting devices through either singlet fission or triplet-triplet annihilation upconversion
45 (TTA-UC)^{11,12}.

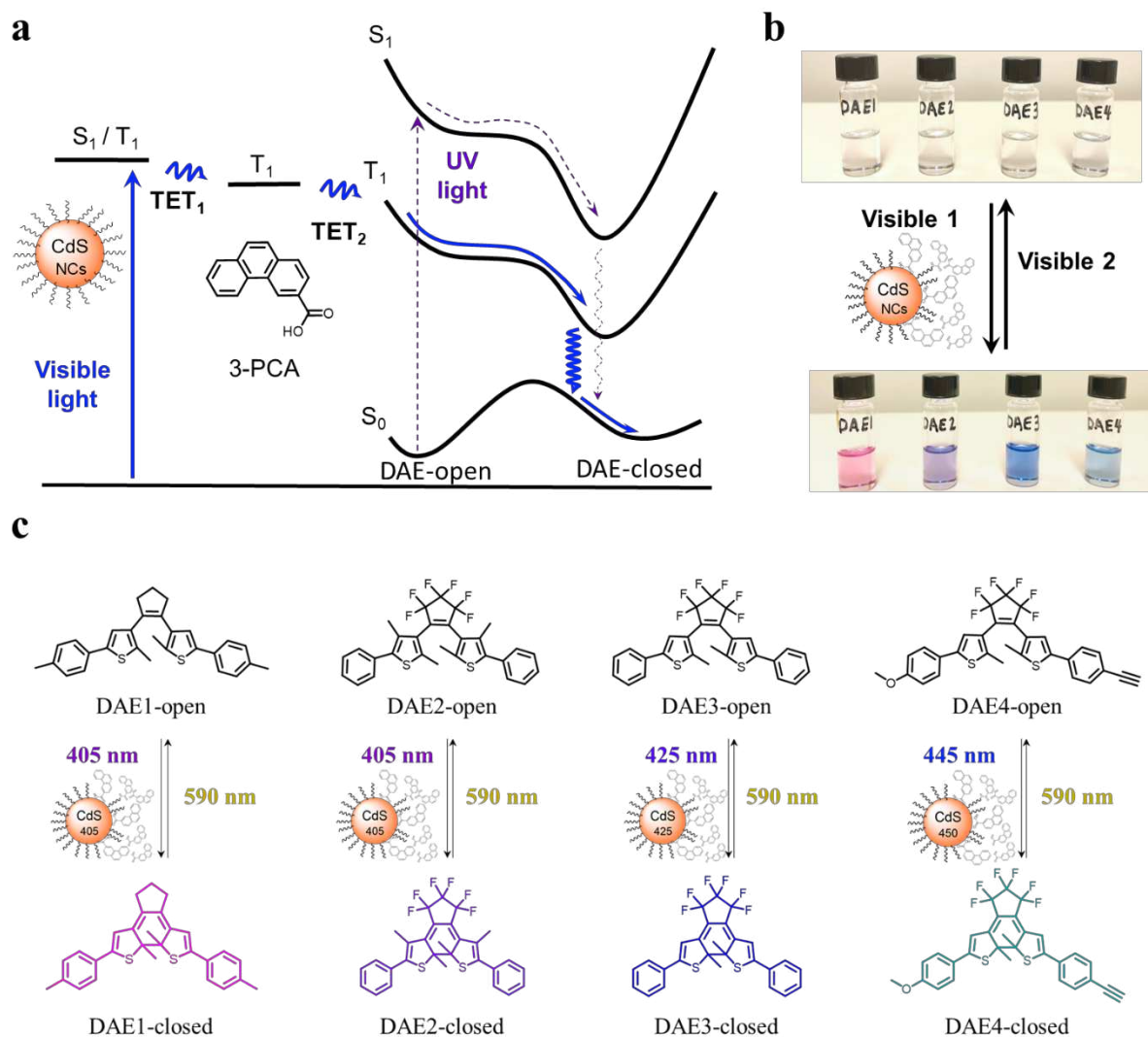
46 Triplet excited states are critical intermediates in many photochemical transformations
47 including photocycloaddition and photoisomerization reactions. Coupling NCs with mediators
48 provides an efficient route to power these photochemical transformations using low energy
49 radiation. Weiss and co-workers recently demonstrated that CdSe NCs can catalyze regio- and
50 diastereoselective intermolecular [2+2] cycloadditions¹³ and that CuInS₂/ZnS NCs catalyze the
51 photoreductive deprotection of aryl sulfonyl-protected phenols¹⁴. However, triplet sensitization

52 from NCs to drive photoisomerization processes at longer and thus less harmful wavelengths
53 remains a largely unexplored area.

54 Photoisomerization is the key photochemical process to operate photochromic
55 molecular switches, often referred to as photoswitches, in which a structural change between
56 two or more isomers is achieved by irradiation with light at different wavelengths¹⁵.
57 Diarylethenes (DAEs)^{16,17}, among the most extensively used molecular switches, have been
58 widely applied as smart materials in constructing optical memories¹⁸, multi-responsive
59 switchable devices¹⁹ as well as in bioimaging²⁰ and photodynamic therapy²¹. Typically,
60 ultraviolet (UV) light is required to induce efficient colorization via ring-closing isomerization
61 (photocyclization) of DAEs. UV light causes photooxidation and thus degradation of the
62 molecular switches and materials thereof. In addition, the penetration depth in tissue is very
63 poor, which is a severe downside considering the potential use of these switches in
64 photopharmacology^{22,23}. Many research efforts have been attributed to design all-visible-light
65 activated DAEs²⁴, such as shifting the absorption spectrum by chemically extending the π
66 conjugation^{25,26}, or using upconverting nanoparticles that absorb in the visible or near-infrared
67 region to generate UV light to drive the photoisomerization^{27,28}. However, directly shifting the
68 absorption band of DAEs requires complicated synthesis, while the low efficiency of the
69 upconverting process leads to overall low photoisomerization efficiencies. Triplet energy
70 transfer from molecular triplet sensitizers has been proven to be another strategy²⁹⁻³³, however,
71 the typical use of molecular sensitizers imposes limitations due to the rather constrained
72 molecular design, relatively weak light absorption and high sensitivity towards oxygen. Thus,
73 it is desirable to develop a general and improved approach that can be applied to a large set of
74 DAEs using visible light only, while maintaining the high efficiency of photoisomerization and
75 excellent fatigue resistance.

76 Our system is based on CdS NCs combined with phenanthrene-3-carboxylic acid (3-
77 PCA) to mediate the TET process, and it demonstrates a simple yet efficient noncovalent
78 strategy to achieve photoisomerization of selected DAEs using light at different wavelengths
79 in the visible region. The mechanism implies triplet-like excited states of the NCs lying only
80 ~20 meV below the strong excitonic absorption band, which can sensitize the ‘dark’ triplet of
81 the surface anchored mediator^{7,34}. Subsequent TET from the mediator to the DAEs drives the
82 photoisomerization along the triplet reaction pathway, as schematically illustrated in Figure 1a.
83 The large absorption cross sections of CdS NCs enable unusually efficient visible light
84 absorption compared to previously reported approaches using molecular sensitizers. The
85 visible absorption band of CdS NCs can easily be tuned by varying the size of the CdS NCs to
86 meet the transparent windows of the relevant DAE derivatives, thereby driving the
87 photoisomerization of diverse DAE photoswitches at desired visible wavelengths. The
88 photoisomerization of our simple non-covalent ‘cocktail’ strategy upon visible light irradiation
89 is as efficient as that of direct UV light irradiation and prevents photodegradation over multiple
90 irradiation cycles. Moreover, the system can be operated both in solution and in the solid state.
91 The switching of our systems can be retained at atmospheric environment, that is, it displays
92 insensitivity to oxygen in the solid state, which is appealing in the fabrication of high-
93 performing all-visible-light activated optoelectronics and memories.

94



95

96 **Figure 1. Schematic mechanism, color change and chemical structures of all-visible-light**

97 **activated photoisomerization of DAEs through triplet energy transfer from CdS NCs and**

98 **3-PCA. a.** Mechanism of the photoisomerization from DAE-open to DAE-closed under visible

99 light irradiation via two triplet energy transfer steps (TET₁ and TET₂), blue lines. The purple
100 dashed lines indicate the direct UV-induced isomerization through the first singlet excited state.

101 **b.** Color changes of DAE derivatives under visible light irradiation in both isomerization

102 directions in the presence of CdS NCs and 3-PCA. **c.** Chemical structures of DAEs. In view of

103 the different absorption (color) of DAEs, CdS NCs with varied absorption bands are used to

104 achieve irradiation at specific visible wavelengths.

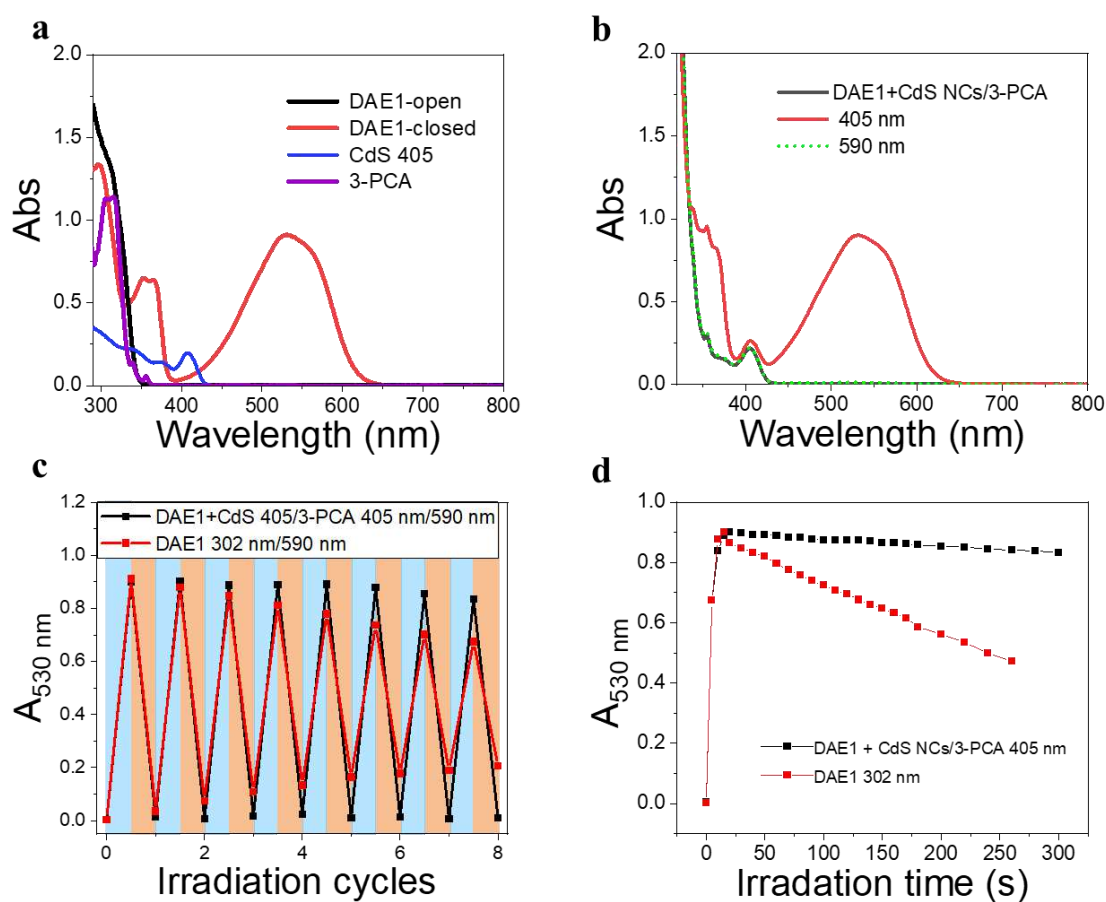
105 **Results**

106 **Materials and Mechanism.** CdS NCs were synthesized according to previous reports^{35,36}, see
107 the details in the Methods/Synthesis section. The growth of CdS NCs during the reaction was
108 monitored by measuring UV-visible absorption spectra of aliquots at different time intervals.
109 Once the first absorption peak of CdS NCs reached the desired wavelength for the visible light
110 irradiation study, the reaction was stopped by quickly cooling the solution to room temperature.
111 Three batches of CdS NCs were prepared with the first absorption peak at 405 nm, 425 nm,
112 and 450 nm, labeled CdS 405, CdS 425, and CdS 450, respectively. Transmission electron
113 microscopy (TEM) images, together with UV-visible absorption and PL spectra of the
114 synthesized CdS NCs are shown in Supplementary Figure 1. 3-PCA was synthesized to mediate
115 the triplet energy of CdS NCs⁹. The carboxylic acid functional group enables the anchoring of
116 3-PCA to the surface of CdS NCs, which leads to efficient harvesting of long-lived 3-PCA-
117 localized triplets. Four DAE derivatives (Figure 1c) purchased or synthesized according to
118 previous reports³⁷⁻³⁹ were used to investigate the photoswitching behavior upon visible light
119 irradiation.

120 All-visible-light switchable DAEs are achieved through TETs from CdS NCs via 3-
121 PCA, as schematically indicated in Figure 1a. Visible light irradiation populates the excited
122 state of the CdS NCs, from where the excitation energy is transferred to 3-PCA via the first
123 step of triplet energy transfer (TET₁). The triplet energy of 3-PCA is then transferred to DAE-
124 open via the second step of triplet energy transfer (TET₂), thereby sensitizing the
125 photocyclization reaction along the triplet state pathway. Compared to directly driving the
126 photocyclization of DAE through the singlet excited state upon UV light irradiation (the dashed
127 purple path in Figure 1a), the energy transfer from the triplet state allows for the use of light at
128 longer wavelength with all the advantages mentioned above.

129 **All-visible-light activated photoisomerization.** To demonstrate the all-visible-light control,
130 we first examined the photocyclization of a DAE derivative referred to as DAE1 (2-bis(2-
131 methyl-5-(*p*-tolyl)thiophen-3-yl)cyclopentene), in the presence of CdS 405 and 3-PCA upon
132 visible light irradiation. Figure 2a shows the individual UV-visible absorption spectra of
133 DAE1-open, DAE1-closed, CdS 405 and 3-PCA in toluene. DAE1-open displays no detectable
134 absorption at wavelengths longer than around 350 nm (black spectrum in Figure 2a). Irradiation
135 of DAE1-open at 302 nm (30 s, see details in Methods/Light sources) leads to the formation of
136 DAE1-closed via the ring-closing isomerization, with the characteristic appearance of an
137 absorption band in the visible region (red spectrum in Figure 2a). Concomitant change of the
138 solution color from transparent to pink is observed. No spectral changes were observed for
139 DAE1-open alone upon 405 nm visible light irradiation (Supplementary Figure 2). This is
140 expected, as DAE1-open displays no detectable absorbance at 405 nm and it is also in
141 agreement with the estimated energy of the singlet excited state (4.2 eV) versus the photon
142 energy at 405 nm (3.06 eV). CdS 405 was used as its first absorption band corresponds to a
143 wavelength where DAE1-open and DAE1-closed have no or very low absorbance. Figure 2b
144 shows UV-visible absorption spectra of the mixed solution of DAE1-open with CdS 405 and
145 3-PCA in deaerated toluene. The spectral features of DAE1 remain unchanged after mixing,
146 indicating that there is no ground state interaction. Due to the high molar absorption coefficient
147 of CdS 405, $\epsilon_{405}=4.0\times 10^5 \text{ M}^{-1}\text{cm}^{-1}$, only 0.5 μM is required to initiate the photoisomerization
148 of 50 μM DAE1 under visible light exposure. Although the concentration of the mediator is
149 100 μM , it is completely transparent for wavelengths longer than 370 nm, see the purple
150 spectrum in Figure 2a. Upon visible light irradiation (405 nm, 120 s), the formation of DAE1-
151 closed follows as manifested by the appearance of an absorption band in the visible region (red
152 spectrum in Figure 2b). The observed changes in the UV-visible absorption spectrum are
153 identical to those observed for DAE1 alone upon direct UV light irradiation. Thus, the

154 photoconversion of DAE1 in the presence of CdS 405 and 3-PCA upon exposure to 405 nm
155 light yields a photostationary state (PSS) identical to that resulting from irradiation of DAE1
156 alone with 310 nm light, that is, 94% DAE1-closed⁴⁰. The photocyclization quantum yield of
157 DAE1 in the presence of CdS 405 and 3-PCA under 405 nm irradiation was determined to be
158 35%, which is comparable to the quantum yield of DAE1 under direct 313 nm UV light
159 irradiation (43%)⁴⁰.



160

161 **Figure 2. UV-visible absorption spectra of visible-light activated photoisomerization of**
162 **DAE1. a.** UV-visible absorption spectra of the individual components: DAE1-open (50 μ M,
163 black), DAE1-closed converted from the open form under 302 nm UV light irradiation (red),
164 CdS 405 (0.5 μ M, blue) and 3-PCA (100 μ M, purple) in toluene. **b.** UV-visible absorption
165 spectra of a mixed solution of DAE1-open (50 μ M), CdS 405 (0.5 μ M), and 3-PCA (100 μ M)
166 in deaerated toluene, before (black) and after light irradiation at 405 nm (120 s, red), and then

167 after 590 nm light irradiation (90 s, green-dot). **c.** Reversibility of the photoswitching of the
168 mixed solution as followed by the absorbance at 530 nm over eight irradiation cycles of 405
169 nm and 590 nm light (black), and DAE1 only over the irradiation cycles of 302 nm and 590
170 nm (red). Note that the maxima and minima truly correspond to the respective PSSs of forward
171 and backward switching. **d.** Evolution of the 530 nm absorbance of DAE1-open in the mixture
172 under 405 nm (black) and DAE1 only under 302 nm (red) irradiation over time.

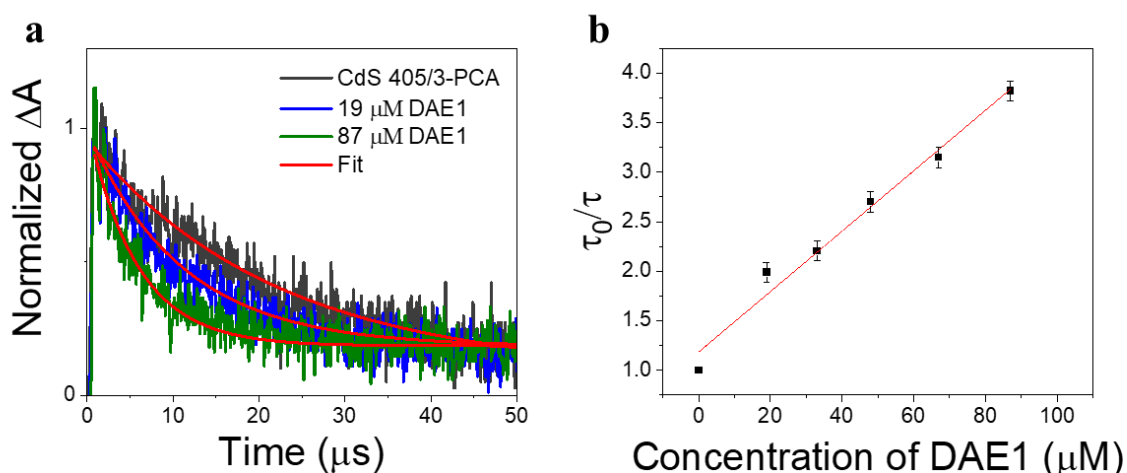
173 Upon subsequent irradiation of the mixed solution with long-wavelength visible light
174 (590 nm) for 90 s, the band in the visible region disappears and the spectrum recovers to the
175 initial state, see green-dot spectrum in Figure 2b. These observations confirm that when DAE1
176 is mixed with CdS 405 and 3-PCA, it can undergo reversible photoisomerization using visible
177 light irradiation, that is, both the ring-opening and the ring-closing reactions are triggered
178 without employing UV light. DAE1 shows fatigue over the switching cycles upon direct UV
179 light irradiation, because of the formation of annulated ring byproducts⁴¹. Over eight irradiation
180 cycles of alternating 302 nm light (30 s) and 590 nm (90 s), nearly 50% degradation was
181 observed (red in Figure 2c). The absorbance evolution also indicates that ~50% DAE1 was
182 degraded over 5 min of constant UV light irradiation (red in Figure 2d). In comparison, over
183 eight irradiation cycles of alternating 405 nm (120 s) and 590 nm (90 s) light exposure, the
184 fatigue resistance of DAE1 is improved (black in Figure 2c), which is also evidenced under
185 long time irradiation experiments (black in Figure 2d). The photoswitching behavior mentioned
186 above indicates that triplet sensitization from CdS NCs and 3-PCA not only provides a strategy
187 to achieve reversible all-visible-light activated DAEs, but can substantially improve the
188 resistance to fatigue as the byproduct is generated mainly on the singlet surface⁴⁰.

189 **Mechanistic investigation of the triplet state sensitization.** As the excited state lifetime of
190 CdS NCs is too short (with an amplitude-weighted average lifetime of ~16 ns, Supplementary
191 Section 3) to directly sensitize the triplet state of DAEs, a mediator that can anchor to the

192 surface of CdS NCs with a long-lived triplet state (on the microsecond or millisecond timescale)
193 is required. The triplet energy of the mediator should be located in between those of CdS NCs
194 and DAE-open. The triplet-like state of CdS 405 is located at about 3.0 eV. The triplet state
195 energies of DAE1-open and DAE1-closed are reported to be 2.5 eV and 0.7 eV, respectively⁴⁰.
196 3-PCA with a triplet state energy (2.6 eV) close to DAE1-open was chosen as the mediator⁹.
197 The efficiency of TET₁ from CdS 405 to 3-PCA was determined to be close to unity (91%, see
198 Supplementary Section 3). In the absence of 3-PCA as the mediator, 405 nm light irradiation
199 did not result in any detectable ring-closing isomerization in a solution of DAE1 and CdS 405
200 (Supplementary Figure 4a). When using phenanthrene as the mediator for CdS 405, no
201 isomerization of DAE1 under visible light irradiation was observed (Supplementary Figure 4b),
202 suggesting that the TET₁ step only occurs when the carboxylic acid group enables anchoring
203 of the mediator to the surface of CdS NCs, because of the short-range Dexter-type triplet energy
204 transfer⁷. When a mediator with a triplet state much lower than that of DAE1-open, such as 1-
205 pyrenecarboxylic acid (PyCOOH, T₁ = 2.0 eV)⁴² was used, no ring-closing isomerization was
206 observed upon 405 nm irradiation (Supplementary Figure 4c) even if efficient TET₁ from CdS
207 NCs to PyCOOH occurred (Supplementary Figure 5).

208 The TET process was further investigated by time-resolved transient absorption (TA)
209 spectroscopy. Our recent work shows that the triplet state of 3-PCA has a broad positive
210 absorption band between 450 nm and 650 nm⁹. 415 nm pulsed laser excitation (2.0 mJ, 10 ns)
211 of CdS 405 mixed with an excess of 3-PCA induced the formation of triplet 3-PCA via the
212 TET₁ step, evidenced by the initial rise in the TA signal at 470 nm (black line in Figure 3a).
213 The subsequent decay of triplet 3-PCA corresponds to a lifetime of 22 μs, consistent with our
214 previous observation⁹. Adding DAE1 to the CdS 405/3-PCA solution results in a decrease in
215 the triplet lifetime of 3-PCA, due to the TET₂ step from 3-PCA to DAE1-open. Figure 3b shows
216 an analysis by the Stern-Volmer equation, $\tau_0/\tau = 1 + \tau_0 k_q [Q]$, where τ_0 and τ are the triplet

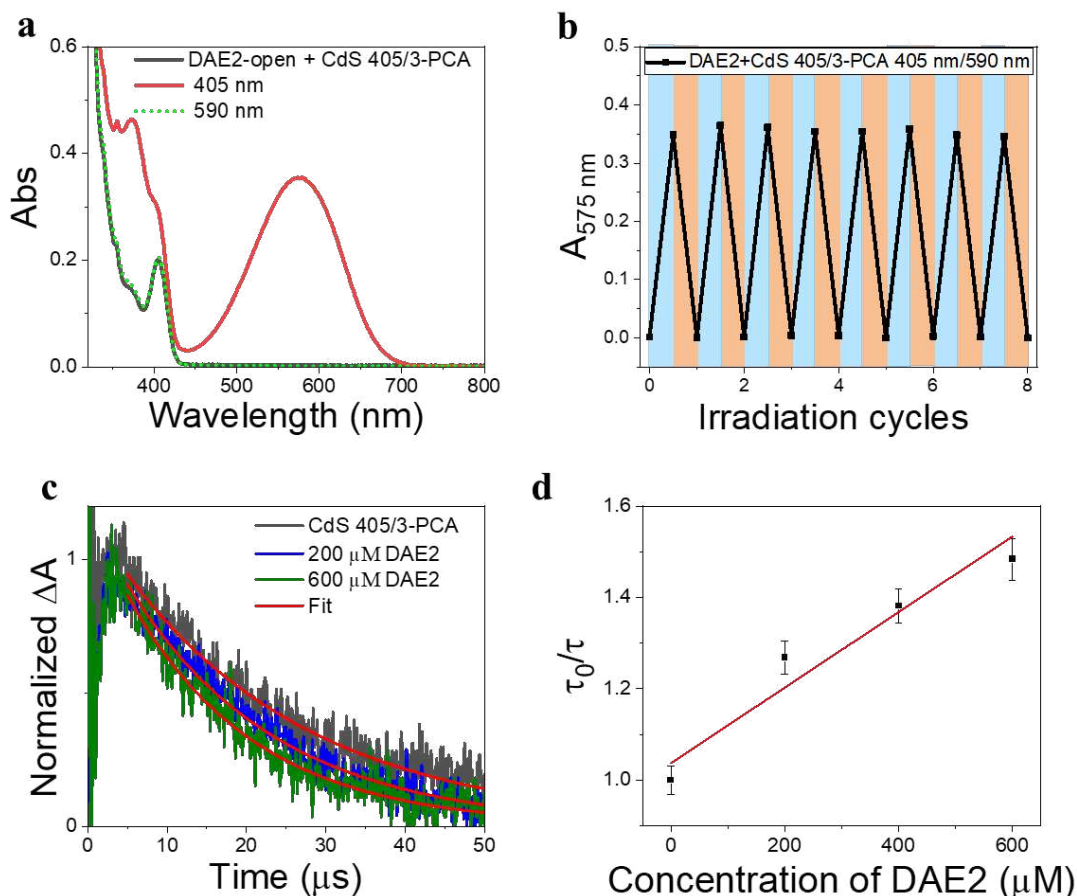
217 lifetimes of 3-PCA without and with DAE1, respectively, k_q is the bimolecular quenching rate
 218 constant, and $[Q]$ is the concentration of the quencher, i.e. DAE1-open. The linear fit of the
 219 Stern-Volmer plot in Figure 3b gives $k_q = 1.4 \times 10^9 \text{ M}^{-1}\text{s}^{-1}$, which is expected for an
 220 efficient diffusion-controlled process. Thus, the TA study demonstrates that the triplet states of
 221 3-PCA formed in the TET₁ step are effectively transferred to DAE1 in the diffusion-controlled
 222 TET₂ step.



223
 224 **Figure 3. Quenching the triplet state of the CdS 405/3-PCA hybrid by adding DAE1. a.**
 225 Time-resolved transient absorption kinetics at 470 nm upon 415 nm pulsed excitation of CdS
 226 405/3-PCA, and CdS 405/3-PCA mixed with DAE1-open in deaerated toluene. **b.** Stern–
 227 Volmer plot and linear fitting for triplet lifetime quenching of CdS 405/3-PCA by DAE1.

228 **General application to DAE derivatives.** Our simple non-covalent cocktail strategy allows the
 229 hybrid of CdS NCs and 3-PCA to be used as a general triplet sensitizer for a variety of DAE
 230 derivatives under all-visible-light control. To demonstrate the general applicability, we further
 231 tested visible-light-activated photoswitching of a commercially available DAE derivative, 1,2-
 232 bis(2,4-dimethyl-5-phenyl-3-thienyl)-3,3,4,4,5,5-hexafluoro-1-cyclopentene (DAE2). The
 233 sample was conveniently prepared by adding DAE2 into the solution of CdS 405 and 3-PCA
 234 in accordance with the procedure for DAE1. Figure 4a shows the UV-visible absorption spectra

235 of the mixed solution and its response to visible light exposure. Upon 405 nm irradiation, DAE2
236 undergoes photoisomerization from the open form to the closed form, evidenced by the
237 formation of the absorption band in the visible region and purple colorization of the sample,
238 see the red spectrum in Figure 4a and the photo in Figure 1b. The photoconversion of DAE2 in
239 the presence of CdS 405 and 3-PCA upon exposure to 405 nm light yields a PSS that contains
240 58% DAE2-closed, which is lower than that of direct UV irradiation at 313 nm (79%)⁴³. We
241 assign this observation to the relatively large spectral overlap between DAE2-closed and the
242 excitation light at 405 nm, resulting in a direct ring-opening reaction on the singlet excited
243 manifold. The photocyclization quantum yield of DAE2 in the presence of CdS 405 and 3-PCA
244 under 405 nm irradiation was determined to be 39%, which is comparable to the quantum yield
245 of DAE2 under direct 313 nm UV light irradiation (46%)⁴³. Upon 590 nm irradiation, the
246 visible band of DAE2-closed disappears and the spectrum completely recovers to the initial
247 state. The all-visible-light activated photoswitching of DAE2 is fully reversible without
248 obvious fatigue as shown in Figure 4b. From density functional theory (DFT) calculations, the
249 T₁ state of DAE2-open is estimated to be 2.8 eV (Supplementary Table 1), about 0.2 eV higher
250 than that of 3-PCA. A triplet energy transfer reaction will occur even under slightly endergonic
251 conditions as described by the Sandros equation⁴⁴ albeit with a slower rate. Triplet quenching
252 experiments of the CdS 405/3-PCA hybrid by DAE2 and Stern-Volmer plot yield $k_q = 2.7 \times$
253 $10^7 \text{ M}^{-1}\text{s}^{-1}$ (See Figures 4c and 4d), which is almost one order of magnitude smaller than that
254 observed for DAE1, in accordance with a less effective TET₂ step due to endergonic triplet
255 energy transfer.



256

257 **Figure 4. UV-visible absorption spectra and triplet quenching of CdS 405/3-PCA mixed**

258 **with DAE2. a.** UV-visible absorption spectra of the solution of DAE2-open (50 μM), CdS 405

259 (0.5 μM), and 3-PCA (100 μM) in deaerated toluene, before and after light irradiation at 405

260 nm (black and red) and then after 590 nm light irradiation (green-dot). **b.** Reversibility of the

261 photoswitching as followed by the absorbance at 575 nm over eight irradiation cycles of 405

262 nm and 590 nm light. **c.** Time-resolved transient absorption kinetics at 450 nm upon 410 nm

263 pulsed excitation of CdS 405/3-PCA and mixed with DAE2 in deaerated toluene. **d.** Stern–

264 Volmer plot for triplet lifetime quenching of CdS 405/3-PCA by DAE2.

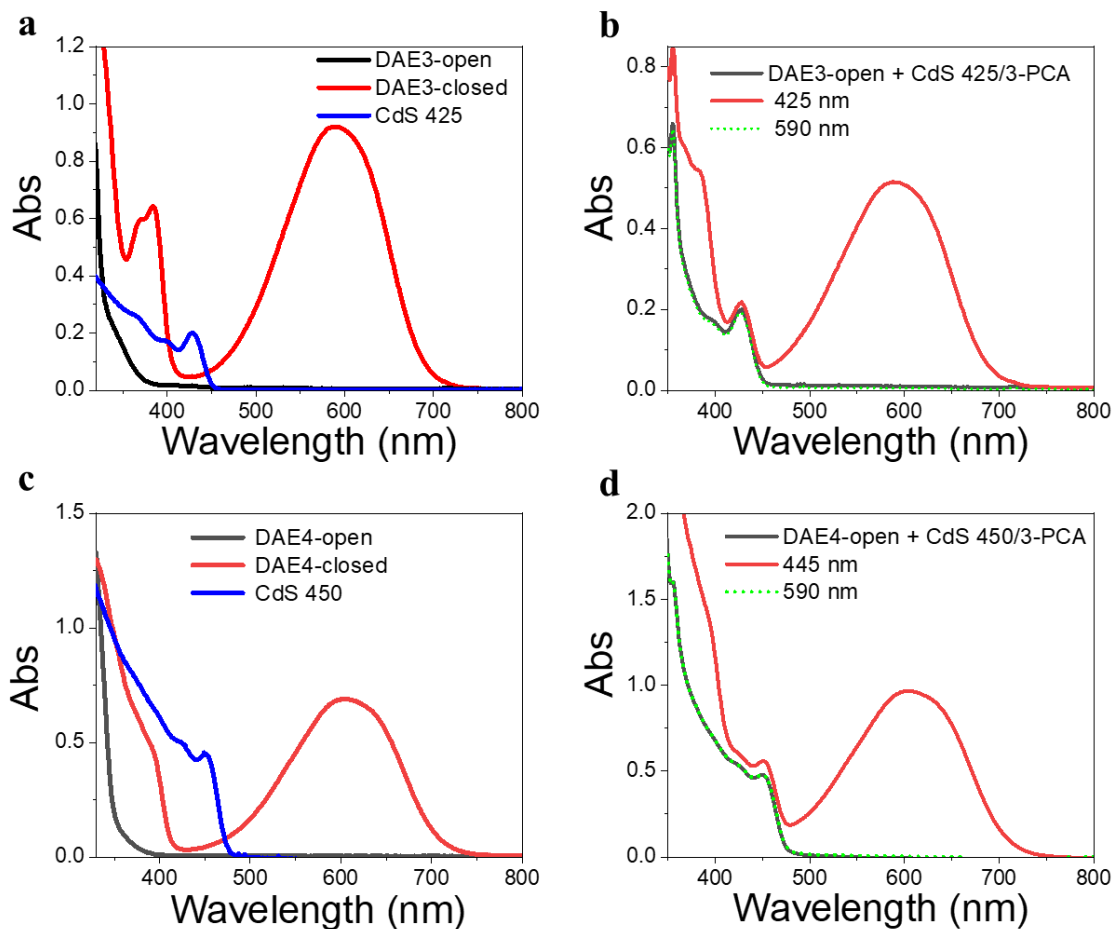
265 Due to the size-tunable absorption of CdS NCs, it is possible to selectively activate the

266 photoisomerization also of other DAE derivatives in the desired visible wavelength window

267 where both the ring-open and closed form are more or less transparent. As a demonstration,

268 herein we used two other DAE molecules, referred to as DAE3 and DAE4, respectively. The

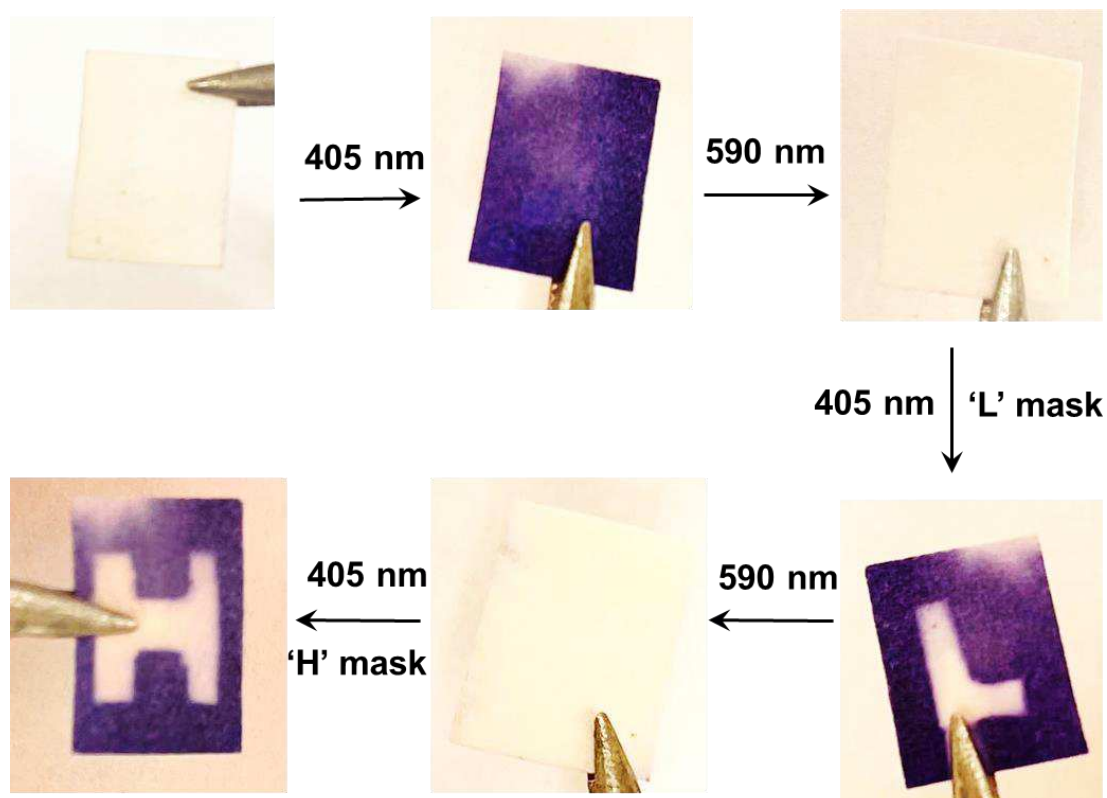
269 wavelength window for these two derivatives allows for convenient excitation at 425 nm and
270 445 nm, respectively, as seen in Figures 5a and 5c. Direct irradiation at 425 nm and 445 nm of
271 the samples containing DAE3-open alone and DAE4-open alone, respectively, did not result
272 in any ring-closing photoisomerization (see Supplementary Figure 6). CdS 425 and CdS 450
273 were synthesized to meet the absorption at the above-mentioned wavelengths (blue spectra in
274 Figures 5a and 5c), and were used for the purpose of all-visible-light switching of DAE3 and
275 DAE4. Figure 5b shows UV-visible absorption spectra of DAE3 mixed with CdS 425 and 3-
276 PCA in deaerated toluene. Upon 425 nm visible light irradiation, the formation of DAE3-closed
277 was evidenced by the appearance of the typical visible absorption band and the color of the
278 solution changed to blue, see the red spectrum in Figure 5b and the photo in Figure 1b. Figure
279 5d shows the corresponding spectra of DAE4 mixed with CdS 450 and 3-PCA. Indeed,
280 irradiation at 445 nm clearly triggers the photocyclization reaction for DAE4, as shown again
281 by the appearance of the absorption band in the visible region and the solution color changed
282 to cyan, see the red spectrum in Figure 5d and the photo in Figure 1b. After subsequent
283 irradiation at 590 nm of the mixed solutions, the visible bands of DAE3 and DAE4 disappeared,
284 and the spectra recovered to their initial states (green-dot spectra in Figures 5b and 5d). The
285 above-mentioned observations illustrate that the ring-closing photoisomerization of a variety
286 of DAE derivatives can be activated at desired visible wavelengths by simply varying the sizes
287 of CdS NCs, and the all-visible-light photoswitching processes are fully reversible.



288

289 **Figure 5. UV-visible absorption spectra of two DAE derivatives under tunable visible**
 290 **irradiation. a.** Individual UV-visible absorption spectra of DAE3-open (50 μM , black),
 291 DAE3-closed (formed under UV light irradiation, red), and CdS 425 (0.3 μM , blue) in toluene.
 292 **b.** UV-visible absorption spectra of the mixed solution of DAE3-open, CdS 425, and 3-PCA in
 293 deaerated toluene, before and after irradiation at 425 nm (pulsed laser, 10 min) and then after
 294 590 nm light irradiation (60 s). **c.** Individual UV-visible absorption spectra of DAE4-open (50
 295 μM , black), DAE4-closed (formed under UV light irradiation, red), and CdS 450 (0.5 μM , blue)
 296 in toluene. **d.** UV-visible absorption spectra of the mixed solution of DAE4-open, CdS 450,
 297 and 3-PCA in deaerated toluene, before and after light irradiation at 445 nm (continuous laser,
 298 9 min) and then after 590 nm light irradiation (60 s).

299 **All-visible-light switching in the solid state.** Our excitation strategy also performs well in the
300 solid state. A solid sample was prepared by soaking a piece of filter paper in a solution
301 containing CdS 405, 3-PCA, and commercially available DAE2, with the same concentrations
302 that were used for the UV-visible absorption study. The solvent slowly evaporated at 60 °C in
303 the dark. Different patterns can be generated and erased reversibly on this solid sample as
304 demonstrated in Figure 6. Initially, the dry sample paper is white, and 405 nm light irradiation
305 stimulates a white-to-purple color change of the entire paper. Subsequent irradiation with
306 visible light at 590 nm fully reverses the color change. Moreover, the patterns of ‘L’ and ‘H’
307 shapes can be written and erased consecutively using masks on the same paper by simply
308 altering between the two visible wavelengths. Although the TET reactions require diffusion to
309 occur, which is limited in the solid state, we hypothesize that the slow evaporation of the
310 solvent can cause the mediator 3-PCA to aggregate around the surface of CdS NCs. This would
311 lead to a local concentration enhancement of the molecules, and the shorter intermolecular
312 distances that follow would still allow for efficient TET reactions to occur, even in the presence
313 of oxygen. We also observed that all-visible-light activated photoisomerization was possible
314 in an air-equilibrated solution (Supplementary Figure 7), although the photocyclization
315 efficiency was a factor of 3-5 times lower than that in the deaerated case. Thus, our strategy of
316 combining CdS NCs, 3-PCA and DAEs in the solid state can be used to generate different
317 patterns reversibly and reproducibly, which holds great potential in all-visible-light responsive
318 materials for optical memory and data storage.



319

320 **Figure 6. All-visible-light switching in the solid state.** Images of a filter paper prepared from
 321 CdS 405, 3-PCA and DAE2 solution, and its subsequent color (white and purple) and pattern
 322 change ('L' shape and 'H' shape), upon visible light irradiation by simply varying the
 323 wavelength between 405 nm and 590 nm in normal atmospheric environment.

324 Discussion

325 In summary, we have demonstrated that the hybrid of CdS NCs and 3-PCA can induce all-
 326 visible-light activated photoisomerization of diarylethene photoswitches through triplet energy
 327 transfer. This represents a novel strategy to achieve all-visible-light controlled photoswitchable
 328 systems at selective wavelengths both in solution and in the solid state, even in the presence of
 329 oxygen. Our systems are prepared by a 'cocktail' approach, that is, simply by mixing the
 330 molecular building blocks and the NCs via non-covalent assembly. The quantum yield of
 331 photocyclization through triplet energy transfer from CdS NCs/3-PCA is almost as high as that
 332 of direct UV light irradiation, and the hybrid system displays better fatigue resistance over

333 multiple irradiation cycles. NCs are par excellence candidates for this approach due to their
334 appealing photophysical properties (high molar absorptivity, small singlet-triplet energy gap,
335 and near unity efficiency of triplet energy transfer). It should be stressed that our strategy is
336 generally applicable to a large variety of DAE derivatives with different absorption spectra and
337 energy levels, due to the ability to precisely adjust the absorption spectra of the NCs by size
338 variations. Further development of DAE derivatives with carboxylic acid functional groups can
339 simplify the current three-component system to a bi-component system by excluding the
340 mediator. Our simple yet effective non-covalent assembly approach paves the way to
341 convenient fabrication of all-visible-light controlled photoswitchable optoelectronic devices
342 and memories. Moreover, in the case of using non-toxic NCs, it should allow to non-invasively
343 address bioactive switches in the context of photopharmacology.

344 **Data availability**

345 The data that support the findings of this study are available from the corresponding authors
346 upon reasonable request.

347 **Methods**

348 **Chemicals**

349 Analytical reagent grade toluene from VWR was used without further purification for spectroscopic
350 measurements. 1,2-bis(2,4-dimethyl-5-phenyl-3-thienyl)-3,3,4,4,5,5-hexafluoro-1-cyclopentene
351 (DAE2) and 1-pyrenecarboxylic acid (PyCOOH) were purchased from TCI. Phenanthrene was
352 purchased from Fluka A.G. The detailed synthesis of 3-PCA, DAE1, DAE3 and DAE4 was according
353 to previous reports^{9,37-39}. CdS NCs were prepared by a slightly modified synthesis according to previous
354 reports^{35,36}.

355 Cadmium oxide, sulfur powder, 1-octadecene, and dioxane were purchased from Sigma Aldrich. Oleic
356 acid was purchased from Alfa Aesar. 3-acetylphenanthrene was purchased from Acros Organics,

357 sodium hypochlorite solution was purchased from Scharlau Chemie, and diethyl ether was purchased
358 from Fisher Chemicals. All the chemicals were used without further purification steps.

359 **Synthesis**

360 CdS NCs: 257 mg of CdO, 6 ml of oleic acid and 15.8 ml of ODE were mixed in a 50 ml three-necked
361 flask, which was degassed under vacuum at 110 °C for 1 hour. After that, the solution was heated to
362 260 °C under N₂ until the mixture turned colorless and clear. 32 mg of sulfur was dissolved in 3 ml of
363 ODE, and degassed under N₂ for 30 minutes, followed by sonication for at least 1 hour. The sulfur
364 solution was injected into the Cd solution at 210 °C. After injection, the solutions were cooled by
365 compressed air to 150-190 °C according to the size required. UV-visible absorption spectra of the
366 aliquots were measured during the reaction. Once the first absorption peak of CdS NCs reached the
367 desired wavelength, the reaction was stopped by fast cooling to room temperature. The obtained CdS
368 NCs were further purified by extraction with hexane/acetonitrile three times and precipitated with
369 acetone twice.

370 **Spectroscopies**

371 UV-visible absorption spectra were measured using a Cary 50 UV-vis-NIR spectrophotometer. Steady-
372 state fluorescence spectra were recorded on a Cary Eclipse fluorescence spectrophotometer.
373 Fluorescence lifetime measurements were carried out using time-correlated single photon counting
374 (TCSPC), which was excited by a 405 nm laser diode (PicoQuant) and recorded by an MCP-PMT
375 detector (10 000 counts, 2048 channels). Time-resolved transient absorption measurements were carried
376 out on a home-built system, in which an Nd:YAG laser (10 ns, 10 Hz, Spectra-Physics, Quanta-Ray)
377 equipped with an OPO (Spectra-Physics, primoScan) was used as a pump beam, and a quartz-halogen
378 lamp was used as a probe light. The time-resolved decays were measured on a 9 stage PMT (Applied
379 Photophysics) coupled with a monochromator (Oriel Cornerstone 130, Newport), and the signals were
380 recorded on an oscilloscope (TDS 2022, Tektronix) communicated with a computer. Transmission
381 electron microscopy (TEM) images were recorded on a Titan 80-300 TEM (FEI Co.) equipped with a

382 monochromator, Cs probe-corrector, and Gatan image filter. The acceleration voltage of the TEM was
383 300 kV.

384 **Sample preparations**

385 All photophysical measurements were carried out in toluene using a 10 mm path quartz cuvette. The
386 samples for UV-visible absorption measurements were prepared by purging with argon for at least 15
387 minutes. The samples for quantum yield and transient absorption measurements were prepared by at
388 least 4 freeze-pump-thaw cycles. The solid sample was prepared by soaking a piece of filter paper into
389 the solution for UV-visible absorption measurement, letting all the solvent slowly evaporate at 60 °C
390 in the dark.

391 **Light sources**

392 302 nm irradiation was performed using a UV analytic lamp ($\sim 10 \text{ mWcm}^{-2}$ at the sample); 425 nm
393 irradiation was carried out by using an Nd:YAG laser (10 ns, 10 Hz) equipped with an OPO set at 425
394 nm (2.0 mJ/pulse); 405 nm irradiation ($\sim 60 \text{ mWcm}^{-2}$) and 445 nm irradiation ($\sim 15 \text{ mWcm}^{-2}$) were
395 carried out by using continuous-wave lasers (Coherent, OBIS) coupled with a concave lens; 590 nm
396 irradiation ($\sim 15 \text{ mWcm}^{-2}$ at the sample) was carried out using an LED light source (LED Engin,
397 FWHM = 20 nm).

398 **Quantum yield and conversion of photocyclization reactions**

399 Photocyclization quantum yields were determined by using Ferrioxalate actinometry (405 nm, $\Phi=1.14$)
400 according to standard methods⁴⁵. 405 nm irradiation was carried out by using a continuous-wave laser
401 (Coherent, OBIS) coupled with a neutral density (ND) filter to reduce the intensity.

402 The conversion of DAE1-open to DAE1-closed at the photostationary state (PSS) was reported as 94%
403 upon 310 nm irradiation⁴⁰, and the molar absorption coefficient of DAE1-closed was determined to be
404 $\epsilon_{522} = 1.97 \times 10^4 \text{ M}^{-1}\text{cm}^{-1}$. The conversion of DAE2-open to DAE2-closed at the PSS was reported
405 as 79% upon 313 nm irradiation⁴³, according to which the molar absorption coefficient of DAE2-closed

406 in toluene was determined to be $\epsilon_{575} = 1.25 \times 10^4 \text{ M}^{-1}\text{cm}^{-1}$. The corresponding conversions at the
407 PSS upon 405 nm light irradiation were calculated using the above molar absorption coefficients.

408 **Computational details**

409 Density functional calculations (DFT) were performed using the Gaussian 16 software package⁴⁶ using
410 the hybrid functional B3LYP and the basis set 6-311+G(d,p). Full optimization of the ground-state
411 structure was followed by excited state calculations using the basis set 6-31G(d). Excited state energies
412 (12 lowest of both triplet and singlet spin) were calculated using the time-dependent formalism
413 (TDDFT).

414 **References**

- 415 1 Alivisatos, A. P. Semiconductor clusters, nanocrystals, and quantum dots. *Science* **271**, 933-
416 937 (1996).
- 417 2 Sun, Q. *et al.* Bright, multicoloured light-emitting diodes based on quantum dots. *Nat.*
418 *Photonics* **1**, 717-722 (2007).
- 419 3 Michalet, X. *et al.* Quantum dots for live cells, in vivo imaging, and diagnostics. *Science* **307**,
420 538-544 (2005).
- 421 4 Dai, X. L. *et al.* Solution-processed, high-performance light-emitting diodes based on quantum
422 dots. *Nature* **515**, 96-99 (2014).
- 423 5 Rossetti, R., Nakahara, S. & Brus, L. E. Quantum Size Effects in the Redox Potentials, Resonance
424 Raman-Spectra, and Electronic-Spectra of Cds Crystallites in Aqueous-Solution. *J. Chem. Phys.*
425 **79**, 1086-1088 (1983).
- 426 6 Wang, X., Zhuang, J., Peng, Q. & Li, Y. D. A general strategy for nanocrystal synthesis. *Nature*
427 **437**, 121-124 (2005).
- 428 7 Mongin, C., Garakyaraghi, S., Razgoniaeva, N., Zamkov, M. & Castellano, F. N. Direct
429 observation of triplet energy transfer from semiconductor nanocrystals. *Science* **351**, 369-372
430 (2016).
- 431 8 Thompson, N. J. *et al.* Energy harvesting of non-emissive triplet excitons in tetracene by
432 emissive PbS nanocrystals. *Nat. Mater.* **13**, 1039-1043 (2014).
- 433 9 Hou, L., Olesund, A., Thurakkal, S., Zhang, X. & Albinsson, B. Efficient Visible-to-UV Photon
434 Upconversion Systems Based on CdS Nanocrystals Modified with Triplet Energy Mediators.
435 *Adv. Funct. Mater.* **31**, 2106198 (2021).
- 436 10 Qin, C. J. *et al.* Triplet management for efficient perovskite light-emitting diodes. *Nat.*
437 *Photonics* **14**, 70-75 (2020).
- 438 11 Tabachnyk, M. *et al.* Resonant energy transfer of triplet excitons from pentacene to PbSe
439 nanocrystals. *Nat. Mater.* **13**, 1033-1038 (2014).
- 440 12 Wu, M. F. *et al.* Solid-state infrared-to-visible upconversion sensitized by colloidal
441 nanocrystals. *Nat. Photonics* **10**, 31-34 (2016).
- 442 13 Jiang, Y. S., Wang, C., Rogers, C. R., Kodaimati, M. S. & Weiss, E. A. Regio- and
443 diastereoselective intermolecular [2+2] cycloadditions photocatalysed by quantum dots. *Nat.*
444 *Chem.* **11**, 1034-1040 (2019).
- 445 14 Perez, K. A., Rogers, C. R. & Weiss, E. A. Quantum Dot-Catalyzed Photoreductive Removal of
446 Sulfonyl-Based Protecting Groups. *Angew. Chem. Int. Ed.* **59**, 14091-14095 (2020).

447 15 Feringa, B. L. & Browne, W. R. *Molecular switches*. 2nd edn, (Wiley-VCH, 2011).

448 16 Tian, H. & Yang, S. J. Recent progresses on diarylethene based photochromic switches. *Chem.*
449 *Soc. Rev.* **33**, 85-97 (2004).

450 17 Irie, M., Fulcaminato, T., Matsuda, K. & Kobatake, S. Photochromism of Diarylethene
451 Molecules and Crystals: Memories, Switches, and Actuators. *Chem. Rev.* **114**, 12174-12277
452 (2014).

453 18 Leydecker, T. *et al.* Flexible non-volatile optical memory thin-film transistor device with over
454 256 distinct levels based on an organic bicomponent blend. *Nat. Nanotechnol.* **11**, 769-775
455 (2016).

456 19 Hou, L. *et al.* Optically switchable organic light-emitting transistors. *Nat. Nanotechnol.* **14**, 347-
457 353 (2019).

458 20 Zou, Y. *et al.* Amphiphilic Diarylethene as a Photoswitchable Probe for Imaging Living Cells. *J.*
459 *Am. Chem. Soc.* **130**, 15750-15751 (2008).

460 21 Hou, L., Zhang, X., Pijper, T. C., Browne, W. R. & Feringa, B. L. Reversible Photochemical Control
461 of Singlet Oxygen Generation Using Diarylethene Photochromic Switches. *J. Am. Chem. Soc.*
462 **136**, 910-913 (2014).

463 22 Velema, W. A., Szymanski, W. & Feringa, B. L. Photopharmacology: Beyond Proof of Principle.
464 *J. Am. Chem. Soc.* **136**, 2178-2191 (2014).

465 23 Broichhagen, J., Frank, J. A. & Trauner, D. A Roadmap to Success in Photopharmacology.
466 *Accounts Chem. Res.* **48**, 1947-1960 (2015).

467 24 Bleger, D. & Hecht, S. Visible-Light-Activated Molecular Switches. *Angew. Chem. Int. Ed.* **54**,
468 11338-11349 (2015).

469 25 Tsvigoulis, G. M. & Lehn, J. M. Multiplexing optical systems: Multicolor-bifluorescent-biredox
470 photochromic mixtures. *Adv. Mater.* **9**, 627-630 (1997).

471 26 Fukaminato, T. *et al.* Molecular Design Strategy toward Diarylethenes That Photoswitch with
472 Visible Light. *J. Am. Chem. Soc.* **136**, 17145-17154 (2014).

473 27 Boyer, J. C., Carling, C. J., Gates, B. D. & Branda, N. R. Two-Way Photoswitching Using One
474 Type of Near-Infrared Light, Upconverting Nanoparticles, and Changing Only the Light
475 Intensity. *J. Am. Chem. Soc.* **132**, 15766-15772 (2010).

476 28 Wu, T. & Branda, N. R. Using low-energy near infrared light and upconverting nanoparticles to
477 trigger photoreactions within supramolecular assemblies. *Chem. Commun.* **52**, 8636-8644
478 (2016).

479 29 Jukes, R. T. F., Adamo, V., Hartl, F., Belser, P. & De Cola, L. Photochromic dithienylethene
480 derivatives containing Ru(II) or Os(II) metal units. Sensitized photocyclization from a triplet
481 state. *Inorg. Chem.* **43**, 2779-2792 (2004).

482 30 Yam, V. W. W., Ko, C. C. & Zhu, N. Y. Photochromic and luminescence switching properties of
483 a versatile diarylethene-containing 1,10-phenanthroline ligand and its rhenium(I) complex. *J.*
484 *Am. Chem. Soc.* **126**, 12734-12735 (2004).

485 31 Fredrich, S., Gostl, R., Herder, M., Grubert, L. & Hecht, S. Switching Diarylethenes Reliably in
486 Both Directions with Visible Light. *Angew. Chem. Int. Ed.* **55**, 1208-1212 (2016).

487 32 Zhang, Z. W. *et al.* Diarylethenes with a Narrow Singlet-Triplet Energy Gap Sensitizer: a Simple
488 Strategy for Efficient Visible-Light Photochromism. *Adv. Opt. Mater.* **6**, 1700847 (2018).

489 33 Zhang, Z. W. *et al.* A building-block design for enhanced visible-light switching of diarylethenes.
490 *Nat. Commun.* **10**, 4232 (2019).

491 34 Efros, A. L. *et al.* Band-edge exciton in quantum dots of semiconductors with a degenerate
492 valence band: Dark and bright exciton states. *Phys. Rev. B* **54**, 4843-4856 (1996).

493 35 Yu, W. W. & Peng, X. G. Formation of high-quality CdS and other II-VI semiconductor
494 nanocrystals in noncoordinating solvents: Tunable reactivity of monomers. *Angew. Chem. Int.*
495 *Ed.* **41**, 2368-2371 (2002).

- 496 36 Li, Z., Ji, Y. J., Xie, R. G., Grisham, S. Y. & Peng, X. G. Correlation of CdS Nanocrystal Formation
497 with Elemental Sulfur Activation and Its Implication in Synthetic Development. *J. Am. Chem.*
498 *Soc.* **133**, 17248-17256 (2011).
- 499 37 Orgiu, E. *et al.* Optically switchable transistor via energy-level phototuning in a bicomponent
500 organic semiconductor. *Nat. Chem.* **4**, 675-679 (2012).
- 501 38 Liddell, P. A., Kodis, G., Moore, A. L., Moore, T. A. & Gust, D. Photonic switching of
502 photoinduced electron transfer in a dithienylethene-porphyrin-fullerene triad molecule. *J. Am.*
503 *Chem. Soc.* **124**, 7668-7669 (2002).
- 504 39 Hermes, S. *et al.* New fast synthesis route for symmetric and asymmetric phenyl-substituted
505 photochromic dithienylethenes bearing functional groups such as alcohols, carboxylic acids,
506 or amines. *Tetrahedron Lett.* **50**, 1614-1617 (2009).
- 507 40 Herder, M. *et al.* Improving the Fatigue Resistance of Diarylethene Switches. *J. Am. Chem. Soc.*
508 **137**, 2738-2747 (2015).
- 509 41 Irie, M., Lifka, T., Uchida, K., Kobatake, S. & Shindo, Y. Fatigue resistant properties of
510 photochromic dithienylethenes: by-product formation. *Chem. Commun.*, 747-748 (1999).
- 511 42 Mongin, C., Moroz, P., Zamkov, M. & Castellano, F. N. Thermally activated delayed
512 photoluminescence from pyrenyl-functionalized CdSe quantum dots. *Nat. Chem.* **10**, 225-230
513 (2018).
- 514 43 Irie, M., Sakemura, K., Okinaka, M. & Uchida, K. Photochromism of dithienylethenes with
515 electron-donating substituents. *J. Org. Chem.* **60**, 8305-8309 (1995).
- 516 44 Sandos, K. Transfer of Triplet Energy in Fluid Solutions III. Reversible Energy Transfer. *Acta*
517 *Chem. Scand.* **18**, 2355-2374 (1964).
- 518 45 Montalti, M. & Murov, S. L. *Handbook of photochemistry*. 3rd edn, (CRC/Taylor & Francis,
519 2006).
- 520 46 Frisch, M. J. *et al.* Gaussian 16, Reversion C. 01e. (2016).

521 **Acknowledgements**

522 We thank Dr. Xiaoyan Zhang and Dr. Shameel Thurakkal for synthesis of 3-PCA, Jutta Schwarz for
523 synthesis of DAE1, and Dr. Shiming Li for synthesis of DAE3 and DAE4. B.A. acknowledges support
524 from the Swedish Energy Agency (contracts: 46526-1 and 36436-2).

525 **Author contributions**

526 L.H. conceived the ideas and designed the project. S.H. and J.A. provided the diarylethene samples.
527 L.H. synthesized CdS NCs. L.H. and W.L. performed the spectroscopy measurements and the data
528 analysis. B.A. performed theoretical calculations. All authors discussed the results and contributed to
529 interpretation of data. L.H. wrote the manuscript with contributions from all authors.

530 **Competing interests**

531 The authors declare no competing interests.

532 **Correspondence**

533 Prof. Dr. Lili Hou^{1,2,3*}
534 orcid.org/0000-0001-9453-4924; Email: lilihou@tju.edu.cn

535 ¹Department of Chemistry and Chemical Engineering, Chalmers University of Technology, Gothenburg
536 412 96, Sweden.

537 ² Present Address: School of Precision Instruments and Optoelectronics Engineering, Tianjin University,
538 Tianjin 300072, China.

539 ³ Present Address: Key Laboratory of Optoelectronics Information Technology, Ministry of Education,
540 Tianjin 300072, China.

541 Prof. Dr. Bo Albinsson^{1*}
542 orcid.org/0000-0002-5991-7863; E-mail: balb@chalmers.se

543 ¹Department of Chemistry and Chemical Engineering, Chalmers University of Technology, Gothenburg
544 412 96, Sweden.

Supplementary Files

This is a list of supplementary files associated with this preprint. Click to download.

- [SIAGeneralApproachforAllvisiblelightSwitchingofDAEsusingNCs.docx](#)